

Algorithm for detection of wave packets in a circular waveguide

Piotr WRZECIONO , Michał SZYMAŃSKI , Hydayatullah BAYAT 

Institute of Information Technology, Warsaw University of Life Sciences, Nowoursynowska 159, bud. 34, 02-776 Warszawa, Poland

Corresponding author: Piotr WRZECIONO, email: piotr_wrzeciono@sggw.edu.pl

Abstract This paper presents an algorithm for detecting wave packets in a circular waveguide. The waveguide terminated with a concrete plug was used to test the method. The concrete was made in accordance with the Eurocode standard. During the tests, a significant difference was observed between the behavior of the speaker and the concrete plug. The pulse reflected from the plug maintained its shape regardless of the sound level. The reflection of the pulse from the speaker's diaphragm resulted in a significant change in the form and duration of the wave packet. These changes were dependent on the sound level of the wave packet. As a result of these modifications was a significant difference between the measurement uncertainty of detecting a pulse reflected from the concrete and the speaker. In the case of reflection from the speaker, an uncertainty of 0.036% was obtained. The smallest measurement error value for the pulse reflected from the speaker was 2.5%.

Keywords: wave packet, detection, waveguide, dispersion, speaker, concrete plug.

1. Introduction

Research conducted in acoustic waveguides allows accurate observations of many phenomena related to sound propagation. A common feature of those experiments is low measurement uncertainty [1, 2]. In addition, it is possible to adapt measurement methods used in optical fibres [3-5]. The paper [6] presents a method for measuring surface reflectance using Gaussian wave packets [6, 7]. The measurement uncertainty of the reflectance obtained by the authors was 0.23% [6]. This low measurement error value meant that further research could be initiated. The primary goal would be to develop measurement automation using the propagation of wave packets in the waveguide.

The study presented here concerns the automatic detection of the beginning of a wave packet, which was generated using a loudspeaker. A pulse of this kind is repeatedly reflected from the waveguide's ends. One is the test sample, while the other is the loudspeaker's diaphragm, which previously generated the impulse. The speaker diaphragm absorbs part of the energy of the wave packet and introduces characteristic distortions of the pulse. One of these is an increase in the duration of the wave packet, which is similar to the dispersion observed in optical fibres [5, 6]. Thus, we decided to design and make a suitable concrete plug to accurately monitor the incident reflections from two different ends of the waveguide. In addition, the time accuracy of the measurements was significantly increased by using audio interfaces operating at a sampling rate of 192 kHz. The high value of sampling frequency allowed us to provide accurate measurements of Gaussian wave packet propagation. Based on these studies, an algorithm for wave packet detection in the waveguide was developed and tested.

2. Measurement stand

To perform wave packet propagation experiments, we developed and built a measurement stand (Fig. 1). The measurement stand was built with the following components: a loudspeaker in a closed enclosure with a waveguide fragment (1), a waveguide made of PVC pipes (2), measurement microphones (flush with the surface) (3 and 4), an audio power amplifier (5), two USB audio interfaces working (6), a laptop computer (7), a concrete plug (8) and a universal meter (9), with a probe to measure the air temperature inside the waveguide. We also used a first-class calibrator with a sound level of 94 dB and a frequency of 1 kHz.

The laptop (AMD Ryzen 7 4800 HQ, 32 GB RAM, RTX 3050Ti) ran under the control of Linux OpenSuSE Tumbleweed. The tasks of the computer were pulse generation and recording. A Jack server [8] was used to control the audio interfaces, allowing to control all parameters of the sound cards. USB audio interfaces

operated at a sampling rate of 192 kHz with 24-bit encoding. We used measuring microphones with omnidirectional polar characteristics, a 1 mV/Pa sensitivity, the equivalent noise level of 20 dBA, and a passband of 12 Hz – 21 kHz (-3 dB relative to sensitivity at 1 kHz). The speaker enclosure (1) was suitably damped inside. The speaker had a diaphragm with a diameter of 11 cm.

The signal from both the first microphone (3) and the second microphone (4) was recorded during the measurement. We ensured that the sound level of the pulse in the waveguide did not exceed 120 dB. None of the microphones recorded a signal greater than 118 dB.

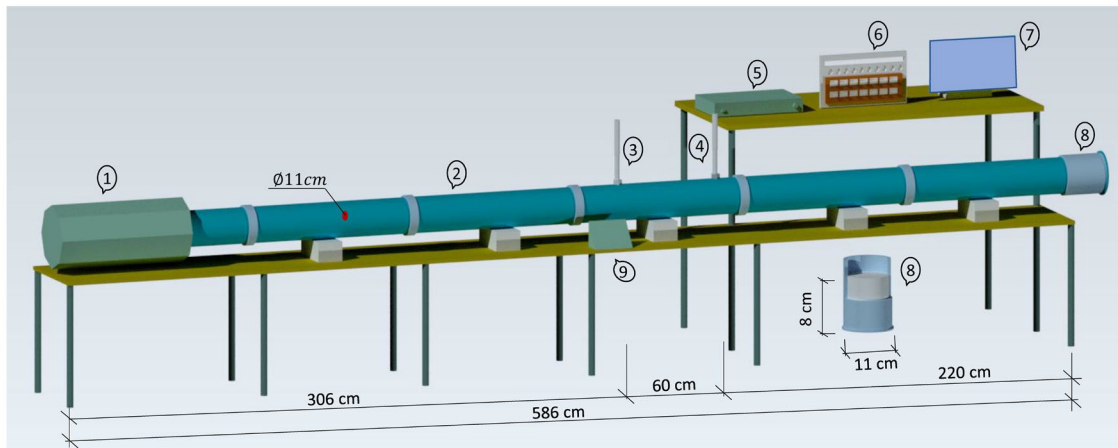


Figure 1. Measurement stand.

The temperature inside the waveguide was measured with a meter having an accuracy of $\pm 0.1^\circ\text{C}$. During all measurements, the temperature inside the waveguide was between 22.1°C and 22.8°C . Inside the laboratory, where the measuring station was located, the temperature was 22°C .

The waveguide was constructed from PVC pipes with a diameter of 11 cm and a density of 1450 kg/m^3 . The chosen PVC pipes had sufficient stiffness and did not vibrate during wave packet propagation. Both 1-meter-long and 2-meter-long pipes were used in the tests. However, no significant differences were observed between the measurement results for a larger number of segments (every 1 m) and a smaller number of elements (every 2 m). This effect is similar to observations from fiber optic measurements, where fiber splices with a shorter length than the propagated wavelength do not significantly affect measurement uncertainty [5].

3. Concrete plug

A concrete sample with a circular cross-section is designed for acoustic wave measurement. The specific shape of the sample allows for limiting wave propagation and consider it without dispersion phenomena. The sample has been designed using normal concrete with the following properties presented in Table 1.

The compressive strength of concrete, denoted as f_{ck} , is a measure of its ability to withstand maximum load before failure. In the case of a concrete cube with dimensions of $15\text{ cm} \times 15\text{ cm} \times 15\text{ cm}$, if it has a compressive strength of 30 MPa after 28 days of curing, it means that it withstood a maximum load corresponding to 30 MPa before failing.

In concrete mix design, the notation “C25/30” is used in accordance with the European standard Eurocode 2 [9] or PN-EN 206 [10]. The letter “C” represents “Concrete” and it indicates the compressive strength class. The “number” represents the characteristic cylinder strength/cube strength of the concrete in megapascals [MPa]. Compressive strength testing of concrete is commonly performed at different intervals, including 3, 7, 14 and 28 days. The specific intervals for early-age compressive strength testing can be varied and specified in the relevant standard or project specifications. The early-age strength measurement provides an indication of the concrete’s early development and can be useful for assessing the progress of construction activities. The standard specifies that the primary measurement for assessing the compressive strength of concrete is at 28 days. This measurement is considered the standard reference point for design calculations, quality control, and acceptance criteria. The compressive strength at 28 days provides a reliable indication of the concrete’s long-term strength and durability.

Table 1. Concrete parameters.

Parameter	Symbol	Unit	Value
Class	C		C25/30
Compressive strength after 28 days	$f_{ck,cub}$	MPa	≥ 30
Density	ρ	kg/m ³	2435.0
Average secant modulus of elasticity	E_{cm}	GPa	31
Plug thickness	h	m	0.08
Radius of plug	R	m	0.055

The modulus of elasticity, also known as Young's modulus, is a mechanical property that describes the stiffness or rigidity of a material [11]. It quantifies how a material deforms when subjected to an applied force or stress. Mathematically, the modulus of elasticity E_{cm} is defined as the ratio of stress to strain within the elastic deformation range:

$$E_{cm} = \frac{\sigma}{\varepsilon}, \quad (1)$$

where E_{cm} is an average secant modulus of elasticity (Young's modulus) of the material, σ is the stress applied to the material, and ε is the strain of material.

In an earlier study [6], we used a plug made of PVC plastic. However, we found that this type of plastic introduces additional distortion during the reflection of the wave packet [6]. So, we decided to make the plug from concrete of a specific type to compare our results with those of other works.

4. Wave packet detection algorithm

4.1. Wave packet

From a previous study related to the propagation and generation of wave packets [6], it was found that the best results were obtained for the Gaussian pulse [7]:

$$x(t) = \exp\left(\frac{-a^2 t^2}{2T_{imp}^2}\right) \sin(2\pi f_0 t), \quad (2)$$

where $x(t)$ is the Gaussian wave packet, T_{imp} is the pulse duration, a is the width factor (default value is 2.5), t is the running time, and f_0 is the fundamental frequency of the wave packet.

In our study, as in the previous one [6], we used wave packets of 5 ms. The frequency f_0 must be chosen so that dispersion due to multimodality does not appear in the waveguide [2, 6, 11-13]. As for the minimum frequency, f_0 should be chosen so that at least one period falls within the pulse [7]. Assuming that the pulse duration is 5 ms, the minimum value of the frequency f_0 is 200 Hz.

The wave packet (2) is its ideal form. In the case of a loudspeaker, the most significant distortion is its elongation caused by the inertia of the transducer [6]. We called this elongation of the pulse duration dispersion of the first kind.

Each reflection of the wave packet from the edge of the waveguide causes a decrease in its energy. As a consequence, its amplitude decreases in proportion to this change. In addition, the speaker introduces a different distortion in the wave packet than is the case with a plug made of concrete. The greater the sound level of the incident wave, the reflected wave packet undergoes another elongation. When designing the algorithm, therefore, it was necessary to consider the nonlinear changes in the wave packet arising during reflection from the speaker diaphragm. We separated the reflection analysis into two parts to assess the mentioned phenomena. The first part describes phenomena with minimal nonlinear distortion content. There are the first wave packet and its reflection from the concrete. The second part analyzes the wave packet reflected from the loudspeaker diaphragm.

4.2. Consideration of wave phase changes

During the reflection of the wave packet from the test sample, a change in the signal's phase can occur [2, 11], which is associated with various wave phenomena. These phenomena are, of course, considered in standards [12, 13]. In the case of detection based solely on changes in dynamic pressure inside the waveguide, this can lead to significant measurement uncertainty. A similar problem exists for measurements in an optical fiber [5]. This type of measurement [5] uses pulse detection using light

intensity levels. It can be similarly implemented in an acoustic waveguide. Then the pulse detection will be independent of the phase change of the signal during reflection. For discrete signals, the signal power is defined by equation [14]:

$$P = \frac{1}{N} \sum_{n=0}^{N-1} |f(nT_s)|^2 = \frac{1}{N} \sum_{n=0}^{N-1} \left| f\left(\frac{n}{f_s}\right) \right|^2 = \frac{1}{N} \sum_{n=0}^{N-1} |f(n)|^2, \quad (3)$$

where P is the power of the signal, T_s is the sampling period, N is the number of samples of the signal, f_s is the sampling frequency, $f(nT_s)$, $f(n/f_s)$, $f(n)$ are designations for the same signal. The power is independent of the signal's phase [14], so relation (3) can be used for pulse detection.

4.3. Wave packet power

To determine the power of a wave packet, calculated according to definition (3), we need its duration and information on possible dispersion. Assuming that we know the pulse time T_{imp} , the amount of dispersion can be calculated as a proportional extension of the wave packet duration:

$$D = \frac{T_{\text{real}}}{T_{\text{imp}}}, \quad (4)$$

where D is the dispersion coefficient, T_{real} is the pulse duration, T_{imp} is the original wave packet duration (2).

In the case of a single wave packet, its duration for the discrete form of the signal will have the following form:

$$M = DT_{\text{imp}}f_s, \quad (5)$$

where M is the number of samples of the discrete wave packet, f_s is the sampling frequency.

In addition to relation (5), it is also essential that the wave packet can start at any time during the entire measurement. Thus, when defining the power of the wave packet subject to detection, it is necessary to include in the reasoning the discrete instant at which the wave packet starts. After taking this into account and using relations (3) – (5), we obtain:

$$P_{\text{puls}}(k) = \frac{1}{M} \sum_{n=k}^{k+M-1} |f(n)|^2 \quad \text{for } 0 < k < N - M, \quad (6)$$

where P_{puls} is the power of the wave packet, N is the number of samples of the entire recorded signal, $f(n)$ is the recorded signal.

4.4. Wave packet sound level

Determining the level of the wave packet is essential because it is relatively easy to exceed the 130 dB limit [2, 11-13]. So, in addition to calculating the power of the wave packet (6), the actual sound level must also be calculated.

The values of the sampled signal are usually given in two ways: as integer binary values or normalized to values between -1 and 1. We do not have directly available information about the actual sound pressure in both situations. To solve this problem, we have to do two things: to have a recorded signal with a known level and the invariability of the audio path settings after registering such a signal.

A signal with a known level can be obtained from an acoustic calibrator. In the case of the measurement microphones used in the experiment, we had no problems applying a first-class calibrator. Such a signal was recorded, and the correction factor was calculated based on it. We labeled the recording of the calibrator signal as $g(n)$. The recording time was a few seconds, as this solution can minimize the measurement uncertainty of such a measurement. The calibrator we had generated a sinusoidal sound with a level of 94 dB and a frequency of 1 kHz. For this reason, this value was taken as a reference. The calculation of the correction was described as follows:

$$L_{\text{norm}} = 10 \log_{10} \left(\frac{1}{N} \sum_{n=0}^{N-1} |g(n)|^2 \right) \quad (7)$$

$$94 = L_{\text{corr}} + L_{\text{norm}}$$

$$L_{\text{corr}} = 94 - L_{\text{norm}}$$

where L_{norm} is the level of the reference signal [dB] sampled normalized in the calculation system, $g(n)$ is the recorded signal from the 94 dB calibrator, L_{corr} is the measurement correction.

Using relation (7) and expression (6), we created an expression to calculate the sound level of the wave packet:

$$L_{\text{imp}}(k) = 10\log_{10}(P_{\text{puls}}(k)) + L_{\text{corr}}, \quad (8)$$

where $L_{\text{imp}}(k)$ is the sound level [dB] at time k , $P_{\text{puls}}(k)$ is the power of the wave packet at time k , L_{corr} is the calibration correction.

4.5. Method

Having worked out all the relationships described earlier, we could define the algorithm and formally perform its implementation and testing. The description is as follows:

- Input data: calibrator recordings R_{cal} (N_1 samples), wave packet recordings R_{wav} (N_2 samples), dispersion coefficient D , ideal wave packet duration, N_{Thread} – the number of a processor's threads.
- Output data: array with indexes of samples with recognized wave packets.
- Method:
 1. Calculate L_{corr} .
 2. Calculate the number of samples per wave packet: M (considering D).
 3. Calculate $L_{\text{imp}}(k)$ for the value of M calculated in step 2.
 4. Set index_maximum to 0, and the number of maxima found K to 0.
 5. Find the maximum of $L_{\text{imp}}(k)$ and store the index value of the sample for which the maximum was found. Additionally, store it as max_last . Start the search with index_maximum . Increase the number of found wave packets by 1 ($K := K + 1$).
 6. Is the value of $\text{max_last} + M$ greater than N_2 ?
 7. If it is less, assign a new value to $\text{index_maximum} := \text{max_last} + M$. and return to step 5. otherwise, go to step.
 8. Output the stored indexes of the maximum.
 9. Terminate the program.
- Computational complexity:
 - In the single-threaded case: $o((M * N_2) + (K * N_2))$, which is of type $o(n^2)$
 - In the multithreaded case: $o((M * N_2)/N_{\text{Thread}}) + (K * N_2)$

4.6. Implementation

The program that implements the method (see Section 4.5) was written in the scripting language for the Octave environment. It is a multi-threaded application run from the command line. A repository containing the entire program code, its description, and the data used in this work was placed on GitHub at: <https://github.com/pwrzec1/Wave-packets-detection.git>.

5. Results

5.1. Testing the wave packet detection program

A Gaussian wave packet (2) with $T_{\text{imp}} = 5$ ms and fundamental frequency $f_0 = 660$ Hz was used during the testing. For these data, only single-mode transmission occurs in the waveguide built on the test bench (Fig. 1). In addition, the frequency of 660 Hz is higher than the resonant frequency of the speaker, which also affects the minimization of nonlinear distortion [15]. However, the increase in pulse time, which is caused by the inertia of the transmitter, cannot be avoided. For example, the results calculated by the program are presented in Fig. 2. The signal was recorded with a first microphone (item 3 in Fig. 1).

The first wave packet (counting from the left) is the incident wave, while the subsequent represents reflections. Odd reflections (the first is the second wave packet) come from the concrete plug. The even reflections come from the speaker's diaphragm. In the figure, several essential phenomena related to the measurement of wave packet propagation can be observed. The first phenomenon is the pulse modification during reflection from the speaker's diaphragm. It is greater the more significant the sound level of the wave packet. With the sound level for the third pulse, dispersion due to the operation of the speaker as a mechanical system is visible.

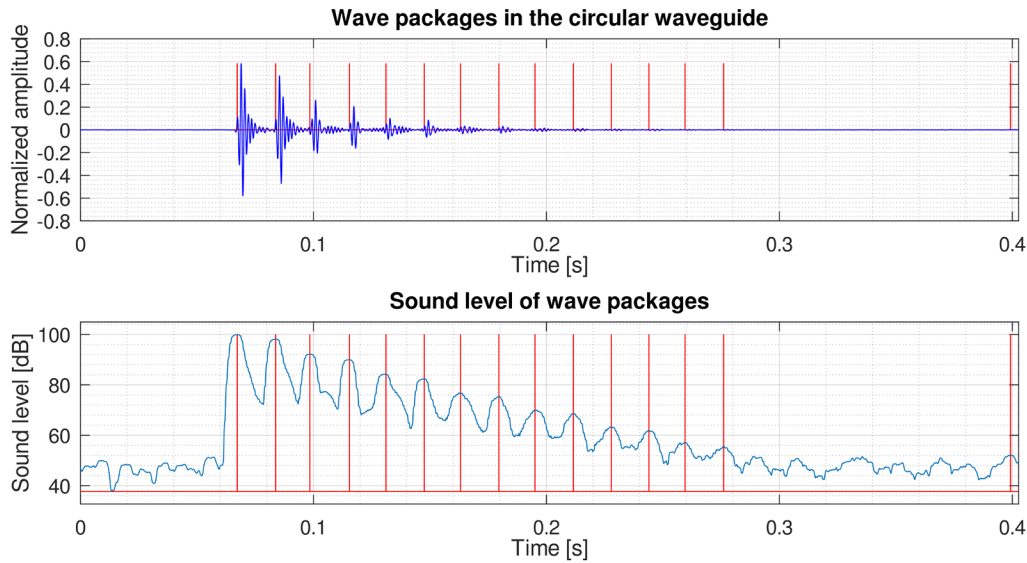


Figure 2. The results of the wave packet detection test calculated for $D = 1$. Vertical (red) dashes indicate the detection of a wave packet.

The apparent relatively high background sound level, from 0.28 seconds onward, is mainly due to the presence of infrasound. Unfortunately, the measurement system (Fig. 1) could not be completely isolated from this type of interference. However, it can be filtered out before calculations are performed.

5.2. Measurement uncertainty of wave packet detection

The detection of wave packet onsets is correct. However, to determine the measurement uncertainty associated with pulse detection, two cases had to be separated for analysis. The first case is a set of reflections from concrete (odd reflections) and from a speaker (even reflections). In addition, it was necessary to study how the algorithm works for different dispersion (D -factor) values and the presence of infrasound in the signal spectrum.

Due to the speaker's distortion in the system, we had to limit the analysis to determining time differences for three pairs from each case (speaker, concrete). In total, this recognizes seven pulses and six-time intervals between them. During the experiment, the temperature in the waveguide and the distances between the ends of the tube and the microphones were kept constant. Thus, in the ideal case, the time interval between pulses should be the same within the same group. In this case, there should be only two-time intervals: T_{concrete} and T_{speaker} . In reality, however, this is not the case, as there are at least two sources of measurement error. The first is the timing inaccuracy of the analog-to-digital converter, which is ± 1 sample. The second is the distortion of the measured pulses caused by the nonlinear operation of the speaker. Thus, dispersion must also be taken into account in the estimation of measurement uncertainty.

We used the mean value and the standard deviation of the time interval to estimate the measurement uncertainty, calculated separately for each subset. The relationships used are shown in the following formulas:

$$\mu_T = \frac{1}{3} \sum_{k=1}^3 N_k, \quad (9)$$

$$\sigma_T = \sqrt{\frac{1}{2} \sum_{k=1}^3 (N_k - \mu_T)^2}, \quad (10)$$

$$r_T = \frac{\sigma_T}{\mu_T} \cdot 100, \quad (11)$$

where μ_T is the mean number of samples between detected pulses, N_k is the number of samples in the k -th interval between pulses, σ_T is the standard deviation of the number of samples between detected pulses, r_T is the relative error of detection of the wave packet [%].

Using formulas (9) – (11), the measurement uncertainty was estimated for D in the range of 0.5 to 2.0, with a step of 0.01. The calculations were carried out for a signal containing infrasound and with

infrasound removed using a high-pass filter. Infrasound was also removed from the calibrator signal recording in the latter case. Figures 3 and 4 show the obtained results.

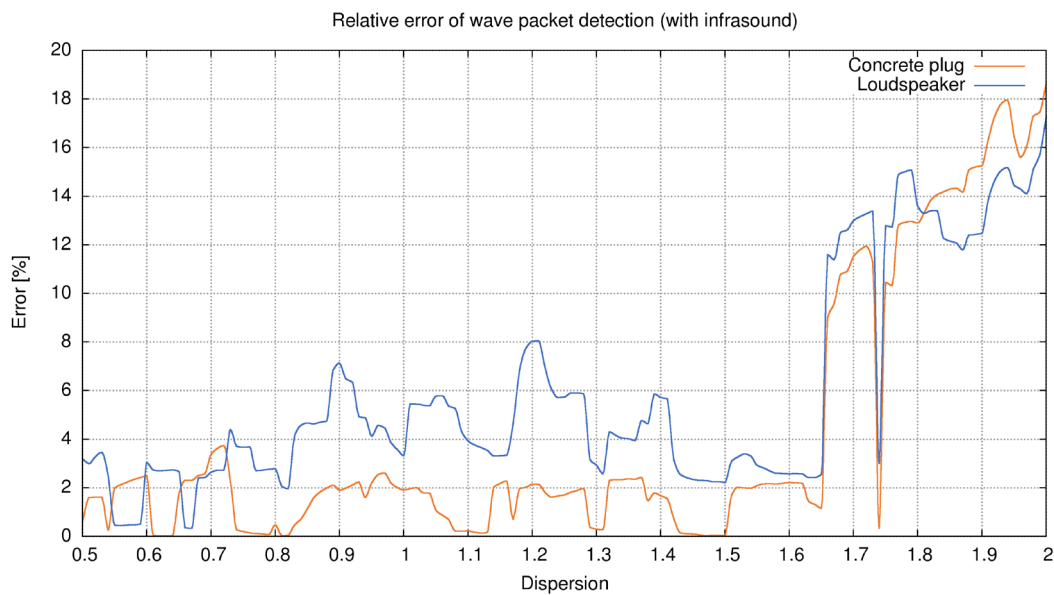


Figure 3. Estimating measurement uncertainty for wave packet detection (recording with infrasound).

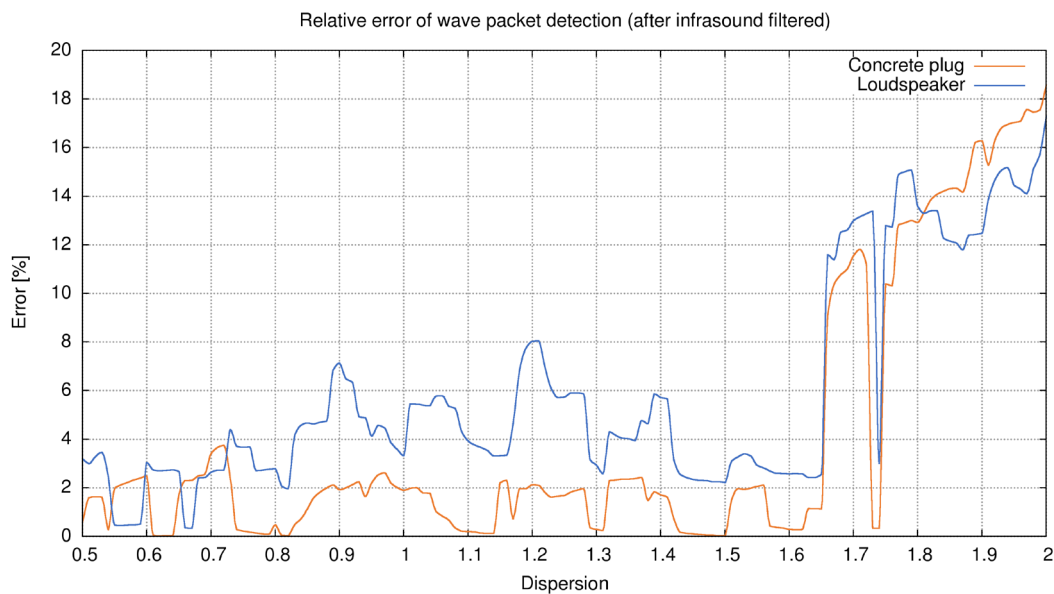


Figure 4. Estimating measurement uncertainty for wave packet detection (recording without infrasound).

Removing infrasound from the signal has increased the ranges for which the measurement uncertainty value is minimal. The minimum error obtained for pulses reflected from a concrete plug was 0.018% ($D = 0.62$), regardless of the presence of ultrasound in the signal. In the case of wave packets reflected from the speaker, the minimum uncertainty value of 0.34% was achieved for $D = 0.67$ (without filtering out the ultrasound). After infrasound filtering, a minimum error of 0.32% was achieved for $D = 0.66$. However, such accuracy is only possible for a single value of D . For dispersion in the range $\langle 1; 1.5 \rangle$, several "windows" are observed in which the error of pulse recognition is little more than minimal. The error values for detecting wave packets reflected from concrete correspond to a discrete sampling error of ± 1 sample.

6. Discussion

In the results obtained, it is noticeable that there is a significant disparity between the detection error of the pulse reflected from the concrete and that reflected from the speaker. The most important factor here is the nonlinear operation of the speaker. Increasing the duration of the pulse, as well as modifying its shape, have a significant impact on the accuracy of the measurement. In the study presented in this paper, the influence of infrasound present in the signal does not significantly affect the measurement results. Regardless of the presence of infrasound, the minimum detection error achieved is within ± 1 sample. This is the absolute limit of the error achievable in discrete systems.

It should be considered whether, due to the error contributed by the speaker to the measurement system, the standards [12, 13] should not be supplemented with a calibration that considers the nonlinearity of the behavior of this transducer. The scatter in the values of reflection and absorption coefficients [6] may be due to the different behavior of the speaker depending on the sound level of the incident wave. However, this is a problem that requires further comparative research.

7. Conclusions

The detection of wave packets in the waveguide presented by us is a solution that enables achieving high confidence in the result possible. This mainly relates to obtaining a very low measurement uncertainty in wave packet recognition (0.02%). This value was achieved for a dispersion coefficient D in the $(1.45; 1.5)$ range. It is a unique solution and will likely make it possible to construct very accurate devices for measuring reflection and absorption coefficients in the future.

Setting up an experimental stand with appropriate samples was necessary to obtain the presented results. The laboratory equipment is also suitable for use in other studies. An additional advantage of the proposed algorithm is that the entire measurement process can be automated and integrated with scientific calculation software, such as Octave or Matlab.

The properties of the concrete, such as density, porosity, and composition, play a role in determining the amount of energy reflected and absorbed. Different materials have varying abilities to reflect or absorb wave energy. The mentioned method exhibits very high accuracy in measurement, as illustrated in Fig. 3 and Fig. 4, which can subsequently be employed to measure concrete with a mixture of different materials, as shown in Fig. 1 (item 8).

Additional information

The authors declare: no competing financial interests and that all material taken from other sources (including their own published works) is clearly cited and that appropriate permits are obtained.

References

1. F. Orduna-Bustamante, F. Arturo Machuca-Tzili, R. Velasco-Segura; Evaluation of the bias error of transmission tube measurements of normal-incidence sound transmission loss using narrow tube reference elements; *J. Acoust. Soc. Am.*, 2018, 144(2), 1040–1048; DOI: 10.1121/1.5051649
2. J. Prusotova, K. Horoshenkov, J.-P. Groby, B. Brouard; A method to determine the acoustic reflection and absorption coefficients of porous media by using modal dispersion in a waveguide; *J. Acoust. Soc. Am.*, 2014, 136(6), 2947–2958; DOI: 10.1121/1.4900598
3. M.K. Barnoski, S.M. Jensen; Fiber waveguides: a novel technique for investigating attenuation characteristics; *Appl. Optics*, 1976, 15(9), 2112–2115; DOI: 10.1364/AO.15.002112
4. A.H. Hartog; *An introduction to distributed optical fibre sensors*; Taylor & Francis (CRC Press), 2017
5. J.P. Dakin, R.G.W. Brown; *Handbook of Optoelectronics: Concepts, Devices, and Techniques, Vol. 1*; Taylor & Francis (CRC Press), 2020
6. P. Wrzeciono, M. Szymański; Measurement of the surface reflectance of an acoustic wave using wave packets propagating in a circular waveguide; *Vibrations in Physical Systems*, 2022, 33(2), 1–8; DOI: 10.21008/j.0860-6897.2022.2.18
7. F. Arickx, J. Broeckhove, W. Coene, P. Van Leuven; Gaussian wave-packet dynamics; *Int. J. Quantum Chem.*, 1986, 30(S20), 471–481; DOI: 10.1002/qua.560300741
8. D. Phillips; Exploring the JACK sound server system - KNOWING JACK; *Linux Magazine*, 2006, 67, 76–82
9. Eurocode 2; *Design of concrete structures*, 2004
10. PN-EN 206+A2:2021-08; *Concrete – Requirements, properties, production and compliance*, 2021

11. F.A. Everest, K.C. Pohlmann; Master handbook of acoustics; McGraw-Hill Education, 2022
12. PN-EN ISO 10534-1:2004; Acoustics – Determination of Sound Absorption Coefficient and Impedance in Impedances Tubes – Part 1: Method Using Standing Wave Ratio, 2004
13. PN-EN ISO 10534-2:2003; Acoustics – Determination of Sound Absorption Coefficient and Impedance in Impedances Tubes – Part 2: Transfer-Function Method, 2003
14. B.P. Lathi; Linear Systems and Signals; Oxford University Press, 2004
15. W. Klippel; Tutorial: Loudspeaker nonlinearities – Causes, parameters, symptoms; Journal of the Audio Engineering Society, 2006, 54(10), 907–939;
<http://www.aes.org/e-lib/browse.cfm?elib=13881>

© 2024 by the Authors. Licensee Poznan University of Technology (Poznan, Poland). This article is an open access article distributed under the terms and conditions of the Creative Commons Attribution (CC BY) license (<http://creativecommons.org/licenses/by/4.0/>).